Available online at www.sciencedirect.com
ScienceDirect
Materials and Design 28 (2007) 2278–2286
Materials & Design
www.elsevier.com/locate/matdes

Electron beam freeforming of stainless steel using solid wire feed

P. Wanjara *, M. Brochu, M. Jahazi

National Research Council, Institute for Aerospace Research, Aerospace Manufacturing Technology Center, 5145 Decelles Avenue, Montreal, Que., Canada H3S 2S4

Received 17 March 2006; accepted 11 August 2006
Available online 7 November 2006

Abstract

The use of electron beam technology for freeforming build-ups on 321 stainless steel substrates was investigated in this work by using 347 stainless steel as a filler metal. The electron beam freeforming studies indicated that line build-ups could be deposited on the substrate material for optimized processing conditions and a slight linear thickening of the re-build occurred as a function of the deposited layer. The evolution in the formation of the Ti (C, N), (Nb, Ti) carbonitrides and Nb (C, N) precipitates was demonstrated to counteract the formation of detrimental Cr-carbides usually observed during welding stainless steels. The mechanical properties of the re-build were similar to the properties of the base metal, showing that homogeneous properties can be expected in the repaired components.

Keywords: (A) Stainless steel; (C) Electron beam freeforming; (D) Wire feed welding

1. Introduction

Freeforming is a relatively new type of component repair or rapid prototyping technique for which a number of solid-freeform-fabrication processes now address the needs of specific sectors of industry. In the aerospace industry, low heat input processes, such as laser and electron beam, are more popular than high heat input processes, such as tungsten inert gas (TIG), for build-up manufacturing on critical and often expensive components due to the stringent structural and mechanical property specifications [1–4]. In particular for the aerospace industry, numerous efforts for freeforming materials have been reported that demonstrate for example the possibility of repairing CMSX-4 single crystals using laser processing [5] and build-ups on Inconel 718 [6], aluminum [7] or Ti–6Al–4V [8] using electron beam welding equipment.

In considering the conditions necessary for manufacturing build-ups for the aerospace industry, both the source and deposition process must be critically selected with the objective of achieving defect-free repair of components. The laser process generally uses filler metal in the form of powder that is spread in front of the advancing beam. However, difficulties related to powder flow from the nozzle can result in important reductions in productivity and/or decrease the build-up quality through the formation of defects such as porosity. With the electron beam welding equipment, the vacuum environment is problematic for the powder feed approach as suction of the filler metal from the feeding nozzle can occur during the air evacuation operation. For this reason, the application of a solid filler metal becomes not only a simpler alternative to loose metallic powder feed, but also has the potential for a higher quality deposit, i.e. build-ups with: (1) lower porosity and (2) fewer inclusions from the natural oxide present at the surface of powder materials for aerospace grades.

However, controlling the interaction between the electron beam and a thin wire in the fusion zone requires particular regulation of the wire feeding rate, angle and height in relation to the beam parameters in order to obtain a sound deposit (Fig. 1). Hence, for application of electron beam freeforming to build-up damaged sections, addressing the role of processing conditions on weld integrity issues is critical because any inherent reduction in the quality of the deposit may prohibit the use of the repaired

* Corresponding author. Tel.: +1 514 283 9380; fax: +1 514 283 9445.
E-mail address: priti.wanjara@cnrc-nrc.gc.ca (P. Wanjara).

0261-3069/$ - see front matter
doi:10.1016/j.matdes.2006.08.008

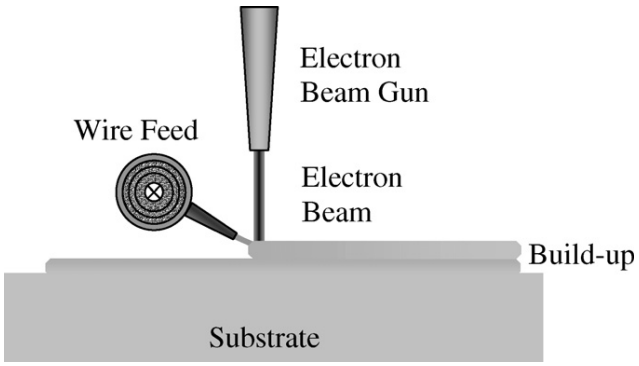

Fig. 1. Schematic drawing of electron beam freeforming process using solid wire feed.

component, especially for the rigorous requirements of the aerospace industry. In this work, the objective was, thus, to investigate the feasibility of using a solid wire as a filler metal for freeforming on a thin gauge substrate and to study the role of the translation speed and wire feed rate on the build-up geometry, effective growth rate, microstructural characteristics and mechanical properties.

2. Experimental method

2.1. Materials

In the present work, the substrate material used for re-build manufacturing was commercially available 1 mm thick sheet of stainless steel 321 (AMS 5510), which contains titanium as a carbide-forming element. The wire filler metal selected for this investigation was 1.1 mm thick stainless steel 347 (AMS 5512), which contains niobium and tantalum as carbide forming elements. These two alloys are classified as stabilized grades because strong carbide formers are added to prevent the formation of chromium carbides, which can lead to sensitization of these materials. The chemical composition of the two alloys used are presented in Table 1.

2.2. Equipment and process parameters

The build-ups on the stainless steel substrates were performed in the vacuum chamber (10^{-6} torr or lower) of a Sciaky W2000 electron beam machine, which has a capability of 60 kV and 42 kW. The beam parameters were adjusted and varied as specified in Table 2 to obtain build-ups 10 cm in length and up to six layers on the edge of the substrate material using the 347 stainless steel wire feed. With increasing thickness of the re-build, the z-axis position of the beam was adjusted to ensure that the working distance and beam focus were constant for each additional layer on the line build-up. The role of the processing conditions on the build-up structure and properties was examined over a processing window for the translation speed of 5.1–15.4 cm min^{-1} and wire feed rates between 12.7 and 37.5 cm min^{-1}. It is noteworthy that the translation speed direction was such that the wire feeding occurred into the leading edge of the molten pool.

Table 2
Electron beam welding parameters used for build-up manufacturing

Parameter	Set point
Accelerating voltage (kV)	25
Beam current (mA)	5
Beam focus	Lower surface of wire feed
Freeforming speed (cm min^{-1})	5.1–15.4
Wire feed rate (cm min^{-1})	12.7–38.1
Working distance (cm)	18

2.3. Sample preparation

Each build-up was first inspected for the occurrence of cracking during processing by liquid die penetration. Then the multi-layer build-ups (roughly 10 cm in length) were cross-sectioned using an abrasive cut-off wheel into 10 individual samples (roughly 1 cm in length) that were mounted in epoxy for metallographic analysis. Specifically, the specimens were ground with successive papers of SiC from 240 grit to 800, followed by rough polishing using 6, 3 and 1 μm diamond suspensions with an alcohol based lubricant on silk cloths and final polishing with 0.05 silica on a porous pad. Etching of specimens was performed by immersion in a solution of 30 ml HCl and 10 ml HNO_3.

2.4. Microstructure evaluation

The characteristics of the build-up samples were examined using optical light microscopy with polarizing capabilities and image analysis software (Clemex Captiva). High-resolution imaging of the build-up microstructures was performed using scanning electron microscopy (JEOL-840) operated in secondary electron imaging (SEI) mode and equipped with energy dispersive spectroscopy (EDAX system) for elemental analysis.

2.5. Mechanical property testing

The microhardness profile across the build-up samples was measured using a dead load of 200 g using a Vickers microhardness tester with a built-in microprocessor for automated determination of the hardness values. For each build-up, an average of at least three hardness values was performed for each location to obtain a nominal microhardness profile for each depositing process condition.

The room temperature tensile properties were determined by the shear punch test method, which is a small-specimen testing technique that enables the characterization of the flow behaviour of the material, including elasticity followed by yielding, work hardening to a maximum stress and fracture [9]. The shear punch test, initially developed for determining the strength and ductility from a small test volume of irradiated material [10], is based on blanking a circular disk from a fixed sheet specimen. In this work, rectangular slices from the substrate and build-up were cut and ground (600 grit SiC finish) to approximately 300–350 μm in thickness and placed between a die and washer assembly fitted on a lower housing. A flat tip cylindrical punch (1.5 mm in diameter), fitted in an upper housing, was forced through the specimen, the action of which punched a circular disk. Since the upper and lower housings, which were fabricated in-house, were attached to a servohydraulic materials testing system, load–displacement data could be obtained from the shear punch testing

Table 1
Nominal composition (wt%) of 321 and 347 stainless steel materials used for the substrate and build-up, respectively

Material	Chemical composition (wt%)										
	C	Cr	Mn	Nb + Ta	Ni	P	S	N	Si	Ti	Fe
Stainless steel 321	0.08	18	2	–	11.0	0.045	0.03	0.044	1	0.15	Balance
Stainless steel 347	0.08	18	2	0.8	11.0	0.045	0.03	–	1	–	Balance

experiments. As correlations between the shear punch data and tensile test data have been identified, the tensile flow properties, including yield strength, ultimate strength and elongation can be determined for various materials from this small-specimen testing technique [11] using the following empirical equation for the strength:

$$\sigma_s^{eff} = \frac{P - P_f}{2\pi r t} = C_s \sigma_t \quad (1)$$

where P (N) is either the yield (P_y) or maximum (P_m) load from the shear load–displacement curve, σ_t (MPa) is the corresponding yield or maximum stress in tension, σ_s^{eff} (MPa) is the effective yield or ultimate stress in shear, P_f (N) is the friction load, r (mm) is the punch radius, t (mm) is the specimen thickness, and C_s is an empirical correlation coefficient that was determined in this work to be 0.54 and 0.64 for the yield and ultimate tensile strengths, respectively.

The empiricial equation used for determining the ductility was [11]:

$$\varepsilon_{eff} = \frac{D_f - D_y}{t} = C_d \varepsilon \quad (2)$$

where D_f is the displacement to fracture, D_y is the displacement to the yield, t is the thickness (mm), ε is the reduction in area (%) and C_d is the correlation coefficient for the ductility that was determined to be 1. Intuitively, this linear equation is satisfying in that $D_f - D_y$ should be zero for a completely brittle material (i.e. no plasticity) and $D_f - D_y$ should approach the specimen thickness (t) for a completely ductile material.

3. Results and discussion

3.1. Macroscopic analysis of the re-build

During re-build manufacturing of the stainless steel substrate, it was determined that the electron beam freeforming process was nearly 100% efficient in the consumption of the solid wire feedstock, which is consistent with previous work on aluminium and titanium alloy deposits [12]. Although the demonstrated deposition rates for electron beam freeforming equipment in this work are 1.5–300 $cm^3\ h^{-1}$, the optimal conditions for re-build manufacturing on the stainless steel substrate was determined to be between 4.8 and 14.3 $cm^3\ h^{-1}$. Under such conditions, each re-build was found to successfully pass die penetrant testing, which demonstrates the possibility of forming crack-free deposits using solid wire feed for freeforming.

Fig. 2 shows a macrograph of a typical six-layer build-up on a 321 stainless steel substrate using 347 stainless steel wire feed. From the side view, the different build-up layers can be distinctively observed, which suggests that excessive heat was not applied and minimal collapse of molten metal occurred over the substrate. After processing, the overall shape of the substrate was conserved and only local mixing at the interface between the wire filler metal and the substrate was observed to occur. Specifically, the cross-section of a build-up given in Fig. 3 shows that the interface between the stainless steel substrate and the filler metal has a rectilinear shape. The interaction or mixing that occurs between the molten metal and the substrate was observed to be between 30 and 40 μm in size, as indicated by the interfacial region in Fig. 3. Previous work on electron beam freeforming of BNi-2 deposits on stainless steel 321 has indicated a smaller interfacial region of approxi-

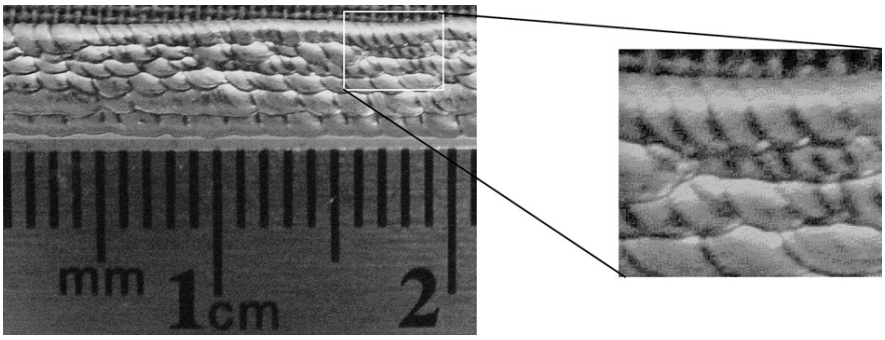

Fig. 2. Macrograph of a six-layer build-up.

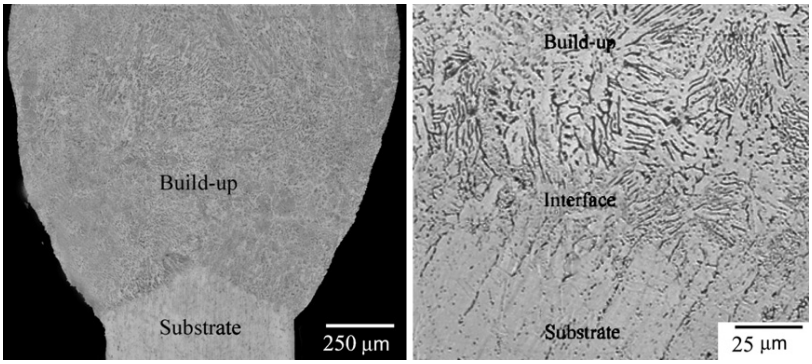

Fig. 3. Micrograph showing the interfacial region between the build-up and substrate.

mately 10 μm [13], which was attributed to the relative differences in the respective melting temperatures that limited the interaction. Hence, the occurrence of a greater interaction and a larger size for the interfacial region during freeforming of the 321 stainless steel substrate with the 347 solid wire is reasonable considering the similarity in the material compositions and melting temperatures.

The variation in the width across a six-layer build-up is illustrated in Fig. 4. After the initial increase in width from the dimensions of the substrate, the size of the deposit was observed to be relatively constant and an average width of 2139 ± 82 μm was measured as delineated in Fig. 4. Analysis of the build-up height as a function of each deposited layer was studied to examine the consistency in growth of the re-build. Fig. 5 shows a linear plot for the average height of the build-up as a function of the number of deposited layers, which enables the modelling of the inter-relationship between the processing conditions during electron beam solid freeform fabrication and the final dimensions of the build-up. On average, the height for a six-layer build-up with one re-melt per layer was found to be 1885 ± 58 μm, which gives a height to width ratio of 0.9. As indicated in Fig. 5, each build-up layer was observed to contribute to an effective growth rate of 327 μm/layer for freeforming conditions of 10 and 25 cm min^{-1} for the translation speed and wire feed rate, respectively. The value for the effective growth rate and height to width ratio is comparable to previous work on electron beam freeforming of BNi-2 deposits on 321 stainless steel which has indicated growth rates between 350 and 430 μm/layer and ratios between 0.5 and 1.0 for defect free build-ups [13].

The influence of the translation speed on the effective growth rate of the build-up as plotted in Fig. 6 indicated an optimum value of 0.33 mm/layer at a translation speed of 10 cm min^{-1}. At a higher translation speed, the lower heat input and lower volume of wire fed into the molten pool produced a lower effective growth rate (0.26 mm/layer) and height to width ratio (0.48) for the deposit. Alternatively, at a lower translation speed, the longer time for interaction of the beam spot with the wire widened the build-up at the expense of height and achieved a slower growth rate of the deposit (0.29 mm per pass) and a lower height to width ratio (0.56). Previous work on electron beam freeforming of 2219 aluminium plate with 2319 aluminium wire has indicated that continuously increasing the translation speed from 40 to 80 cm min^{-1}, while maintaining the beam parameters constant, resulted in the linear deposits experiencing a decreasing taper in the height and width, with the overall reduction in the effective growth rate and height to width ratio [12], which is supports the observations in the present work.

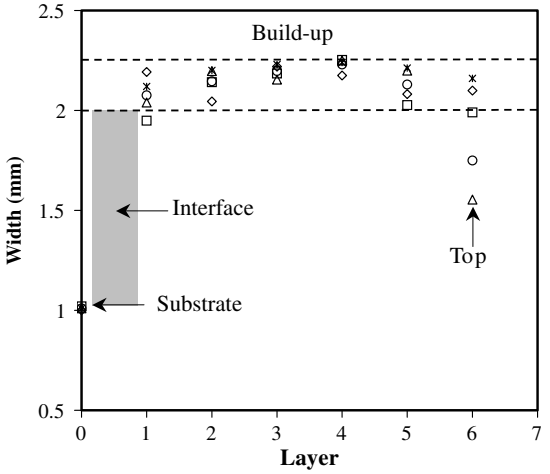

Fig. 4. Width Measurements for a six-layer build-up produced at a translation speed of 10 cm min^{-1} and a wire feed rate of 25 cm min^{-1}.

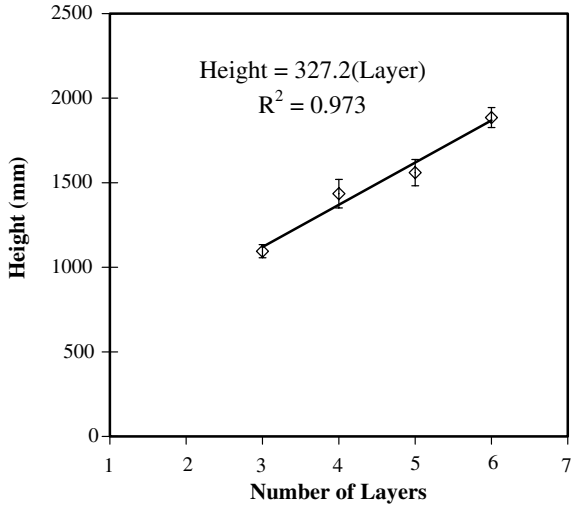

Fig. 5. Build-up height evolution as a function of the number of layers at a translation speed of 10 cm min^{-1} and a wire feed rate of 25 cm min^{-1}.

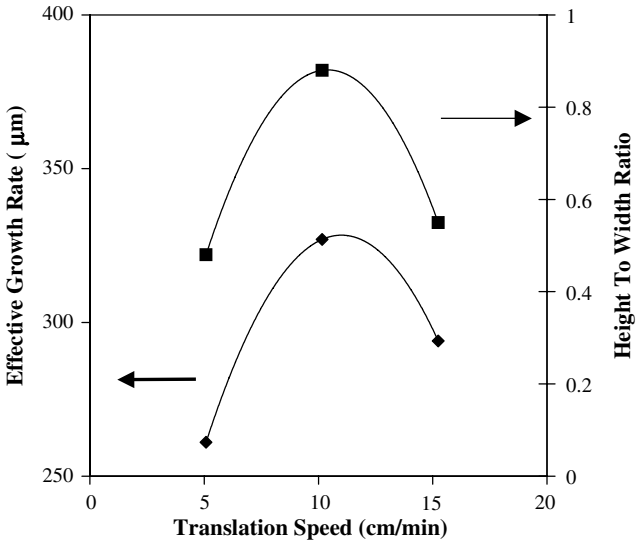

Fig. 6. Effective growth rate and height to width ratio as a function of the translation speed at a constant wire feed rate of 25 cm min^{-1}.

At a constant translation speed of 10 cm min^{-1}, the operating window for the variation in the wire feed rate was observed to be between 20 and 30 cm min^{-1}. Under such conditions the effective growth rate of the deposit was between 0.3 and 0.34 mm/layer and the height to width ratio was 0.72–0.96, as indicated in Fig. 7. At wire feed rate values greater than 30 cm min^{-1} considerable difficulties in producing the build-up were apparent with the occurrence of excessive shifting of the wire relative to the substrate. Alternatively, a wire feed rate below the lower limit of the operating window (i.e. 20 cm min^{-1}) caused the formation of nodular droplets as opposed to a linear deposit on the substrate.

3.2. Microscopic characterization of the re-builds

Analysis of the polished sections of the various build-up layers indicated a continuous interface between the substrate and deposit and defects such as porosity and/or crack formation were not observed. The overall columnar microstructure of the build-up, which consisted of bands of dendrites, as illustrated in Figs. 3 and 8a, was apparent across the entire length of the deposit manufactured with the solid wire feed. The predominantly columnar grains in the microstructure of the deposit were observed to have grown epitaxially towards the heat gradients (Fig. 8b), which is inevitably related to the high cooling rate experienced in the build-up. Previous work has indicated that the highest cooling rate occurs in the liquid ahead of the solid/liquid interface such that at the melting temperature, and just below, the cooling rate approaches 10^3 K s^{-1} for a 316 stainless steel substrate [14,15].

In various locations within the build-up, precipitates possessing a rectangular or square morphology with sizes ranging between sub-microns to few microns were observed. Fig. 9 illustrates representative micrographs of precipitates observed in the deposit layers. X-ray analysis using energy dispersive spectroscopy indicated that the precipitates observed near the interface between the first layer of the deposit and the substrate were composed of titanium, nitrogen and carbon and identified as Ti (C, N) particulates, as illustrated in Fig. 9a. The presence of these particles in the interfacial region between the substrate and the first layer of the deposit is a result of the partial melting and mixing of the substrate material and the solid welding wire feed, since the later only contained niobium and tantalum as carbide formers. The occurrence of Ti (C, N) in this work is supported by previous work on stabilized 321 stainless steel that has indicated an apparent tendency for some solution of carbon in the TiN and some

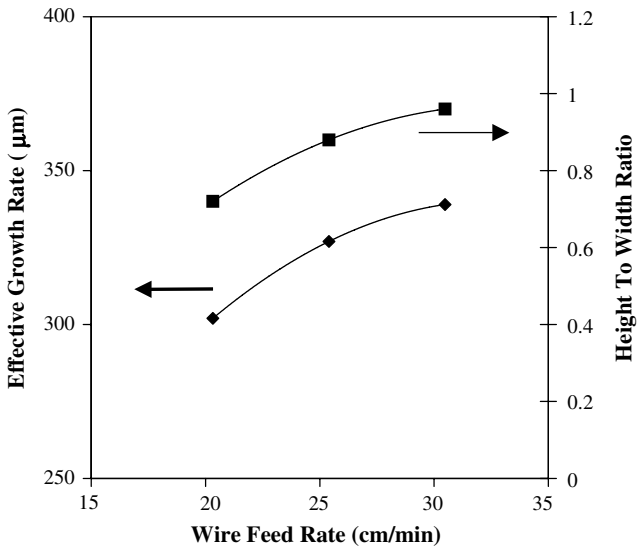

Fig. 7. Effective growth rate and height to width ratio as a function of the wire feed rate speed at a constant translation speed of 10 cm min^{-1}.

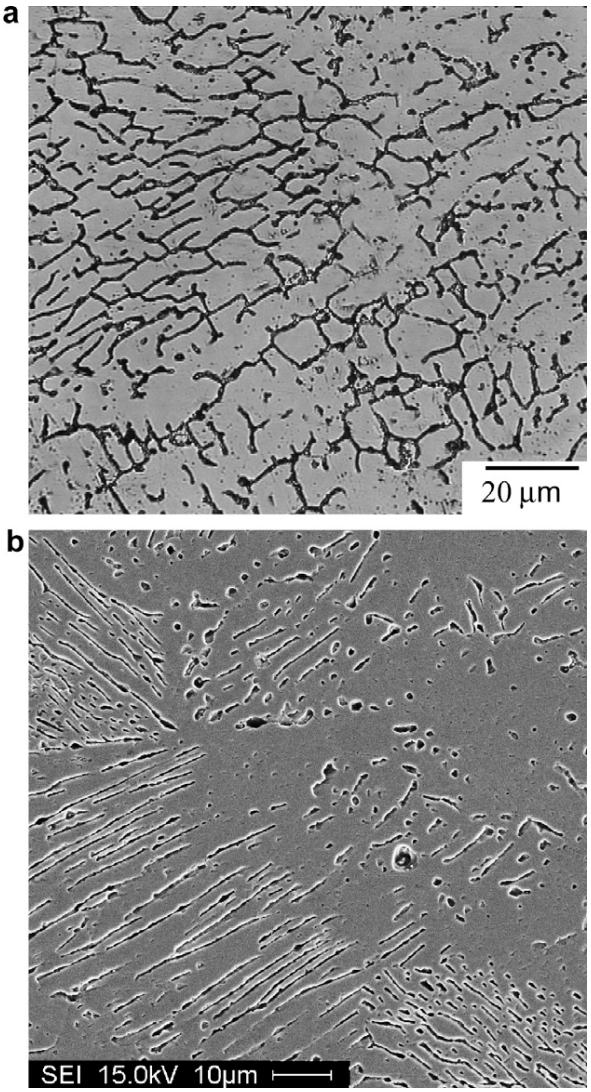

Fig. 8. Microstructure of a six-layer build-up showing: (a) bands of dendrites using optical imaging and (b) columnar grains at the interface between layers using secondary electron imaging.

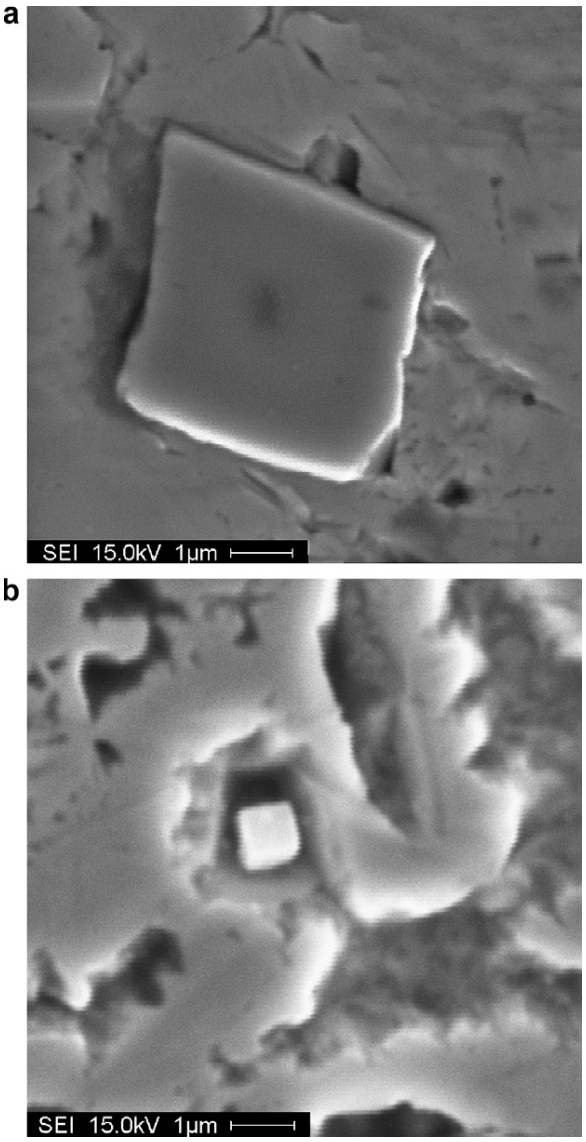

Fig. 9. Representative secondary electron images of: (a) TiC and (b) (Nb, Ti)C precipitates.

solution of nitrogen into the TiC particles, due to comparable lattice parameter values of 4.24 and 4.33 Å, respectively [14,15].

Beyond the interfacial region of the first layer in the deposit, the precipitates were observed to be finer in size (0.5–1 μm) with a cubic morphology, as indicated in Fig. 9b. The respective EDS analyses detected the presence of niobium, titanium, nitrogen and carbon. This suggests that the niobium from the 347 stainless steel welding wire feed and the titanium from the 321 substrate that melted during deposition, combined to effectively trap the carbon and nitrogen into (Nb, Ti) carbonitride complexes. In the subsequent layers, the EDS analysis of the precipitates showed an increase of the Nb concentration at the expense of Ti, which is inevitable due to the dilution effect of the re-melting process. Beyond the fourth layer of the deposit, no measurable traces of titanium were detected in the precipitates, which were identified to be Nb (C, N). Previous work on 321 and 347 stainless steels has indicated considerable miscibility between the MC carbides (TiC, NbC, ZrC, HfC, VC and TaC) due to the sub-stoichiometric characteristics of the precipitates, which thus explains the interlacement of the niobium and titanium within the particles formed in the build-up [16]. In addition, the presence of MC carbides in stabilized steels, even for very low carbon contents, show two types of distribution: (i) a coarse dispersion, 1–10 μm in size, of primary particles formed during solidification; and (ii) a fine dispersion, 5–500 nm in size, of secondary precipitates [15,17–19], which support the range of particle sizes (0.3–7 μm) observed in the present work for the Ti (C, N), (Nb, Ti) carbonitride complexes and Nb (C, N) precipitates.

It is noteworthy that the occurrence of chromium carbide precipitation was not observed in the substrate, at the interface between the substrate and the deposit, or within the various layers of the re-build. Independent of the location analysed in the build-up, the presence of Ti (C, N), (Nb, Ti) carbonitride complexes and/or Nb (C, N) particles indicates that the previous layers were exposed to a temperature higher than the critical solvus temperature for Cr-carbide precipitation [20]. Specifically, it has been found that significant amounts of $Cr_{23}C_6$ can form during re-heating to temperatures of 650–750 °C in non-stabilized stainless steel compositions [16]. In this work, the presence of titanium and/or niobium (M) in the build-up appears to be sufficient in producing a stabilized deposit as indicated by the precipitation of more stable MC carbides resulting from the dissolution of the Cr-carbides ($M_{23}C_6$). In addition, as the critical solvus temperature[1] of the (Ti, Nb) carbonitride precipitates, which is between 1148 and 1219 °C, is greater than that of the Cr-carbides, the MC particles have inherently greater stability relative to the $M_{23}C_6$ particles and the occurrence of sensitization will be inhibited during re-building of additional layers for component repair and/or under operating conditions. Hence, the strategy for build-up manufacturing on 321 stainless steel materials with 347 stainless steel wire feed is similar to that commonly applied for welding of the former grade using the latter as the filler metal. Specifically titanium in type 321 is an element that is not readily recovered during deposition, so that it is not available when needed during solidification to prevent chromium carbide precipitation [21]. However niobium in type 347 remains more effectively in the molten pool, and, prevents sensitization through the precipitation of Nb (C, N) in preference to chromium carbides [21]. Therefore, the build-up of multi-layers with

[1] The equations used to calculate the temperature are $\log_{10}[Nb][C] = 4.55 - (9350/T)$ and $\log_{10}[Ti][C] = 4.55 - (8900/T)$ [16,20]

347 stainless wire feed on a 321 stainless steel substrate will perform better in corrosive environments or in rigorous service conditions such as in the aerospace industry for aircraft exhaust manifolds, stacks and collector rings and fuel and hydraulic lines.

3.3. Mechanical properties of the re-builds

Fig. 10 illustrates the averaged hardness profiles measured across the length of two six-layer build-ups, starting from the interfacial region adjacent to the substrate material. As observed in the hardness profiles, significant changes in hardness values were not apparent across the length of the build-up. The average hardness values for the six layer build-ups were determined to be 165.5 ± 2.6 HV and 167.1 ± 2.2 HV for the two profiles illustrated in Fig. 10. A similar analysis of the hardness for substrate material indicated an average of 159.7 ± 4.2 HV. The hardness specification for an annealed 321 stainless steel (AMS 5510) sheet is 157 HV [22], which is similar to the value determined in this work for the substrate material. For 347 stainless steel (AMS 5512), the material data for sheet, plate or bar stock indicate values of 167 HV for an annealed microstructure [22], while 347 type welding wire feed has been reported to have hardness values of 150–210 HV [23,24] and an as-welded hardness of 169 HV [25]. Hence, the hardness values obtained in the present work for the six-layer build-ups correspond closely with the reported data for grade 347 stainless steel in general. Therefore, no significant difference in the hardness value was obtained between the parent material and the re-build, as expected from material specification information on these grades.

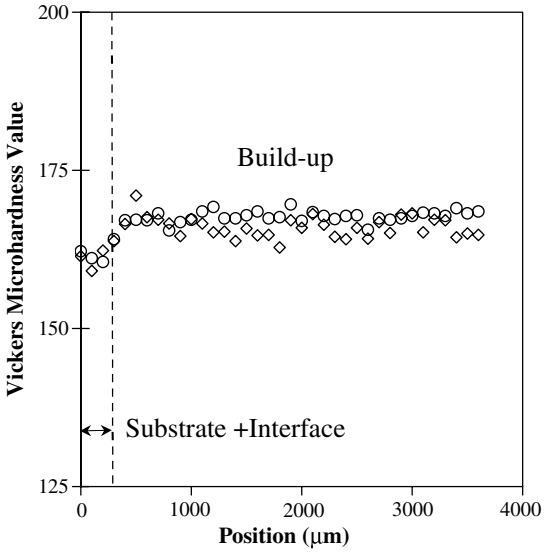

Fig. 10. Profile of the average hardness value on two six-layer build-ups.

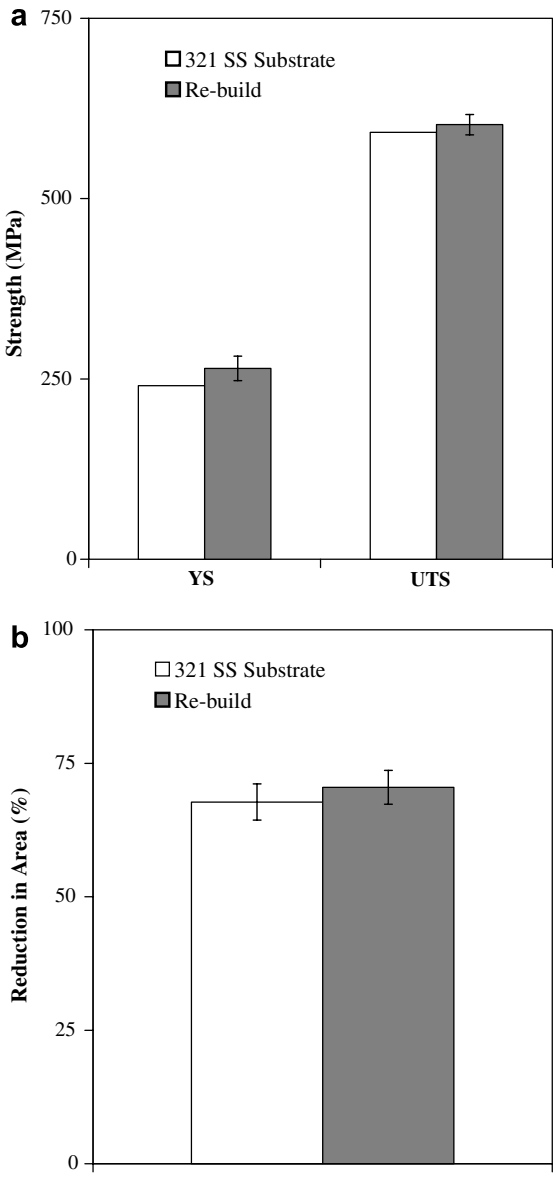

Fig. 11. Tensile properties of the re-build using shear punch testing: (a) yield and ultimate tensile strength data and (b) reduction in area data.

The mechanical properties as determined by shear punch testing of the substrate and build-up materials are given Fig. 11. For the 321 stainless steel substrate and the 347 build-up region, yield and ultimate tensile strength values of 240 and 591 MPa and 265 and 602 MPa were determined, respectively, as indicated in Fig. 11a. The reduction in area values for the 321 stainless steel substrate and the type 347 build-up region were determined to be 68% and 71%, respectively (Fig. 11b). From these results, the tensile strength data for re-build were observed to be similar to the substrate material, which is supported by the hardness values obtained in the present work and the similarity in the mechanical properties of 321 and 347 stainless steels as indicated in Table 3 for different microstructural conditions [22,26–30].

Table 3
Comparison of the mechanical property data for 321 and 347 materials under different microstructural conditions

Property	Present Work		Literature				
	321 Substrate	347 Deposit	Annealed 321 [22,25]	Annealed 347 [22,25]	Clad 347 [27]	Welded 347 [28]	Welded 347 [26,29]
Yield strength (0.1%), MPa	242	265	240	240			
Yield strength (0.2%), MPa					355	318	441–476
Tensile strength, MPa	591	602	585	620	590	565	600–648
Elongation (%)			55%	50%	54%	48%	44–49%
Reduction in area	68%	71%	65%	65%		72%	50–70%

4. Conclusions

Defect-free electron beam freeforming was demonstrated by depositing a 347 stainless steel wire on the edge of a 321 stainless steel thin plate. The increase in height of the repair as a function of the number of layers was approximately linear and a height to width ratio of roughly 0.9 was possible. The microstructure evolution showed that the typical carbides observed in stabilised grades of austenitic stainless steels were present, thus minimising the possibility of sensitization of the repaired region. In addition, the mechanical properties of the re-build were observed to be comparable to that reported in literature for type 321 and 347 stainless steels.

Acknowledgements

This work was conducted under project 46M3-I003-E/L in the Metallic Products Group of the Aerospace Manufacturing Technology Center (AMTC) of the NRC Institute for Aerospace Research (IAR). The authors thank Aerospace Welding Inc., Canada for supplying the SS 321 substrate material and the SS 347 wire filler metal.

References

[1] Vitek JM, David SA, Boatner LA. Microstructural development in single crystal nickel base superalloy welds. Sci Technol Weld Joi 1997;2:109–18.
[2] Mattheij JHG. Role of brazing in repair of superalloy components-advantages and limitations. Mater Sci Technol 1985;1:608–12.
[3] Taminger KMB, Hafley RA, Dicus DL. Solid freeform fabrication: an enabling technology for future space missions. Keynote lecture for 2002 international conference on metal powder deposition for rapid manufacturing, Metal Powder Industries Federation, San Antonio, TX; 2002. p. 51–60.
[4] Taminger KMB, Hafley RA. Electron beam freeform fabrication: a rapid metal deposition process. In: Proceedings of the 3rd annual automotive composites conference, Troy, Michigan, September 9–10, 2003, CD-ROM.
[5] Gäumann M, Bezencon C, Canalis P, Kurz W. Single-crystal laser deposition of superalloys: processing-microstructure maps. Acta Mater 2001;49:1051–62.
[6] Matz JE, Eagar TW. Carbide formation in alloy 718 during electron-beam solid freeform fabrication. Metall Mater Trans A 2002;33A:2559–67.
[7] Taminger KMB, Hafley RA, Fahringer DT, Martin RE. Effect of surface treatments on electron beam freeform fabrication aluminum structures. In: Proceedings of the 15th solid freeform fabrication symposium, Austin, TX, August 2–4, 2004. p. 460–70.
[8] Wallace TA, Bey KS, Taminger KMB, Hafley RA. A design of experiments approach defining the relationships between processing and microstructure for Ti–6Al–4V. In: Proceedings of the 15th solid freeform fabrication symposium, Austin, Tx, August 2–4, 2004. p. 104–15.
[9] Lucas GE. The development of small specimen mechanical test techniques. J Nucl Mater 1983;117:327–9.
[10] Lucas GE. Review of small specimen test techniques for irradiation testing. Metall Trans A 1990;214:1105–19.
[11] Elwazri AM, Wanjara P, Yue S. The effect of microstructural characteristics of pearlite on the mechanical properties of hypereutectoid steel. Mater Sci Eng A 2005;404:91–8.
[12] Taminger KMB, Hafley RA. Characterization of 2219 aluminum produced by electron beam freeform fabrication. In: Proceedings of 13th SFF symposium, 2002. p. 482–89.
[13] Wanjara P, Brochu M, Girard S, Jahazi M. Electron beam freeforming on type 321 stainless steel using BNi-2 brazing paste. Mater Sci Tech 2005;21:613–8.
[14] Lampman S. Weld integrity and performance. Materials Park: ASM International; 1997. p. 89.
[15] Grot AS, Spruiell JE. Microstructural stability of Ti-modified type 316 and type 321 stainless steel. Metall Trans A 1975;6:2023–30.
[16] Padilha AF, Rios PR. Decomposition of austenite in austenitic stainless steels. ISIJ Int 2002;42:325–37.
[17] Padilha AF, Schanz G, Anderko K. Precipitation behavior of titanium-stabilized 15Cr–15Ni–1Mo–Ti–B austenitic stainless steels. J Nucl Mater 1982;105:77–92.
[18] Kou S. Welding metallurgy. 2nd ed. New Jersey: Wiley; 2002. p. 437.
[19] Leitnaker JA, Bentley J. Precipitate phases in type 321 stainless steel after aging 17 years at 600 C. Metall Trans A 1977;8A:1605–13.
[20] Stone PG, Orr J, Guest JC. Metallurgy of Alloy 800. J British Nucl Energy Soc 1975;14:25–34.
[21] Welding Advisers; 2005. Available from: http://www.welding-advisers.com/Welding-stainless.html.
[22] Aerospace Specifications Metals Inc.; 2005. Available from: http://www.aerospacemetals.com/stainless-steel.html.
[23] US Welding Corporation; 2005. Available from: http://www.uswel-dingcorp.com/tds/tds5680.htm.
[24] Outokumpu Stainless, Avesta Welding, Welding Consumables; 2005. Available from: http://www.outokumpu.com/upload/documents/technical/datasheets/272101GB.pdf.
[25] J.W. Harris Company; 2005. Available from: http://www.jwharris.com/images/pdf/347.pdf.
[26] A.M. Castle and Co.; 2005. Available from: http://www.amcastle.com/Download/QG160F.pdf.
[27] Yamamoto H, Yamamoto E, Kojima I, Okazaki T, Okaniwa T, Aihara T. Reheat cracking sensitivity and hydrogen effect on mechanical properties of type 347 stainless steel weld metal. In: Proceedings of the fitness-for-service evaluation in petroleum and

fossil power plants, ASME/JSME joint pressure vessels and piping conference, San Diego, CA, vol. 380; 1998. p. 279–90.
[28] Klemetti K, Hänninen H, Kivilahti J. The effect of sigma phase formation on the corrosion and mechanical properties of Nb-stabilised stainless steel cladding. Weld J 1984;63:17s–25s.
[29] Nassour A, Bose WW, Spinelli D. Creep properties of austenitic stainless-steel weld metals. J Mater Eng Perform 2001;10: 693–8.
[30] Lincoln Electric; 2005. Available from: http://content.lincolnelectric.com/pdfs/products/literature/c610.pdf.